

Thermal analysis of Cu-14.82 wt% Al-0.4 wt% Be shape memory alloy

Canan Aksu Canbay · Ayşe Aydoğdu

Received: 26 April 2012 / Accepted: 19 October 2012 / Published online: 9 November 2012
© Akadémiai Kiadó, Budapest, Hungary 2012

Abstract In the present study, the transformation temperatures and shape memory effect of the Cu-14.82 wt% Al-0.4 wt% Be shape memory alloy were studied. The structural properties of the alloys were characterized by X-ray diffraction. The crystal structure analysis of the alloy shows a thermoelastic transformation from an ordered parent-phase of DO₃ type to the M18R martensite. The microstructure of the alloy was investigated by optical micrographs. The transformation temperatures, enthalpy and entropy values of the alloy were determined by differential scanning calorimetry. Thermogravimetric and differential thermal analysis measurements were performed to obtain the ordered–disordered phase transformations. The activation energy values determined from two different methods were found to be 306.53 kJ mol⁻¹ for Kissinger and 298.57 kJ mol⁻¹ Ozawa.

Keywords Shape memory alloys · Transformation temperatures · Enthalpy · Entropy · CuAlBe

Introduction

Shape memory alloys (SMAs) are an interesting class of functional materials due to their unique thermomechanical

behavior. This behavior has been extensively investigated because of its potential applications. The distinct properties of SMA, as pseudoelasticity, two-way shape memory effect, rubber-like behavior, and high damping capacity, are closely related to the thermoelastic martensitic transformation. These properties make the shape memory alloys (SMAs) a comprehensive smart material. Copper-based shape memory alloys have been received a high attention because of their good shape memory properties associated with the martensitic transformation, low cost, and relatively simple processing [1–4]. In Cu-based alloys, the β -phase is the equilibrium-phase at higher temperatures, but it can be retained as a metastable-phase at lower temperatures by means of a quenching and during quenching, these alloys get configurationally ordered. The decomposition of the β -phase at temperatures below 565 °C involves complex transformations. The phase equilibria in the binary Cu–Al system is one of the basic systems constituting the ternary Cu-based shape memory alloys. In the Cu–Al system, the β -phase with the bcc A2 structure undergoes a two-stage order–disorder transition: A2 (disordered bcc, Cu)-B2 (CuAl)-DO₃ (Cu₃Al) as shown in Fig. 1 [5–7].

In general, the martensitic transformation of high β -phase in Cu-based alloys is responsible for the shape memory effect. But the martensitic transformation start temperature (M_s) for Cu–Al SMA is too high for the applications. Thus, the addition of a third element such as Be, Mn, and Ni, which has supported by recent studies, is effective in stabilizing the β -phase and lowering the martensitic transformation start temperature (M_s). Especially, small amounts of Be addition into Cu–Al binary system are resulted in an important decrease of M_s , –114 K each 1 at.%, without a change in nature of the martensitic transformation. The decrease in M_s extends the temperature

C. Aksu Canbay (✉)
Department of Physics, Faculty of Science, Firat University,
Elazig, Turkey
e-mail: caksu@firat.edu.tr

A. Aydoğdu
Superconductivity and Thermal Analysis Laboratory,
Department of Physics, Faculty of Science, Gazi University,
Ankara, Turkey

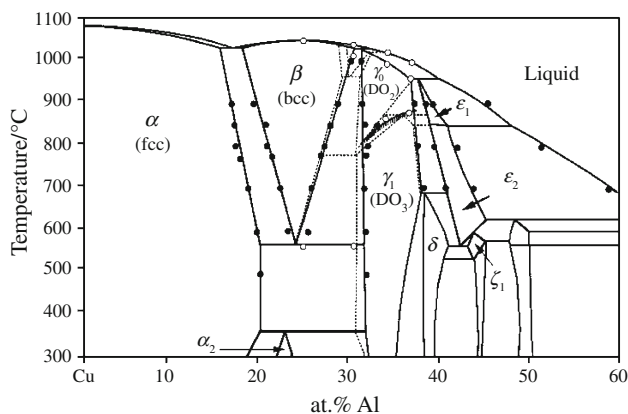


Fig. 1 Phase diagram of the Cu–Al system [4]

range of the alloy and makes Cu–Al–Be an interesting smart system [8, 9]. In particular, β -phase of Cu–Al–Be seems to undergo an ordering transition directly from A2 to DO₃ structure. Moreover; this transformation is appeared as a first-order type and the β -phase is stable higher than 577 °C for eutectoid composition containing approximately 23 at.% Al and 3 at.% Be. It can be retained at room temperature by means of convenient cooling and possessing an ordering reaction to a DO₃ structure at temperature close to 527 °C. Under slow cooling rates, the metastable β -phase decomposes into the phases α (fcc structure) and γ_2 (Cu₉Al₄ structure), with low and high Al contents, respectively. Cu–Al–Be alloy exhibits a martensitic transformation from DO₃ structure to 18R structure at low temperatures [4, 10–12].

The aim of present study is to investigate the microstructure, martensitic transformation temperatures, and phase transitions of Cu–Al–Be shape memory alloy.

Experimental

The studied alloy was prepared from a high purity of Cu, Al, and Be powders (with the proportion of Cu–11.5wt% Al–0.5wt% Be) by melting them in an induction furnace in argon atmosphere. The melting process was repeated for the homogenization of the ingot. Then, the ingot was quenched to 15 °C.

Inductively coupled plasma optical emission spectrometry (ICP-OES) analysis was made to determine the mass proportions of the elements in the alloy. ICP-OES was operated under suitable conditions, including choosing the suitable wavelength for each element Al (396 nm), Be (313 nm), and Cu (324 nm). The phases present in the as-quenched sample at room temperature were analyzed using a X-ray diffraction (XRD) technique. The microstructure and the morphology of the sample were

studied using an optical microscopy. The samples were etched using a solution which consisted 50 g (FeCl₃·6H₂O)–960 mL methanol with 200 mL HCl for optical analysis. The transformation temperatures of the alloy were determined using a differential scanning calorimeter (DSC) with heating/cooling rates of 10, 15, 20, and 25 °C min^{−1}. The TG/DTA measurement was performed from room temperature to 1,100 °C at a heating rate of 20 °C min^{−1} to observe the phase transitions at higher temperatures.

Results and discussion

The mass percentages of the elements in the Cu–Al–Be SMA were determined by ICP-OES analysis. According to the ICP-OES analysis, the proportion of the elements in the alloy was found to be Cu–14.82 wt% Al–0.4 wt% Be. XRD measurement of the as-quenched sample was taken at room temperature using Cu K α ($\lambda = 1.5405 \text{ \AA}$) radiation, and the diffraction patterns of the alloy are given in Fig. 2. As seen in Fig. 2, the as-quenched sample consists of parent-phase and precipitate-phase at room temperature. The diffraction peaks of the alloy are (0 0 18), (2 0 6), and (1 2 0). The peak of (0 0 18) belongs to the martensite-phase. The peak of (2 0 6) indicates the presence of a precipitate-phase at room temperature. The crystal structure of the alloy is monoclinic with the lattice parameters of $a = 4.443 \text{ \AA}$; $b = 5.169 \text{ \AA}$, and $c = 37.012 \text{ \AA}$. The ratio of a/b was calculated to be 0.86 and this value is equal to $\sqrt{3}/2$. This confirms that the parent-phase is ordered and has 18R long period stacking order structure. This means that during the rapid cooling high temperature β -phase is expanded into a DO₃ ordered structure and can further be transformed into a martensite-phase of 18R microstructure [13–16].

As seen in optical micrographs of the alloy, the Cu–14.82wt% Al–0.4wt% Be alloy exhibits a martensite

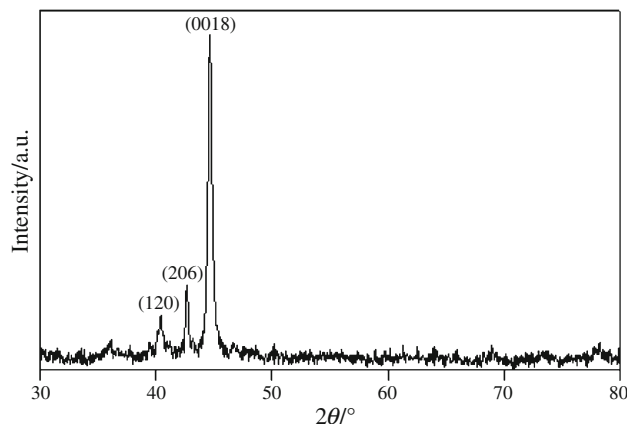


Fig. 2 The X-ray diffraction patterns of the alloy

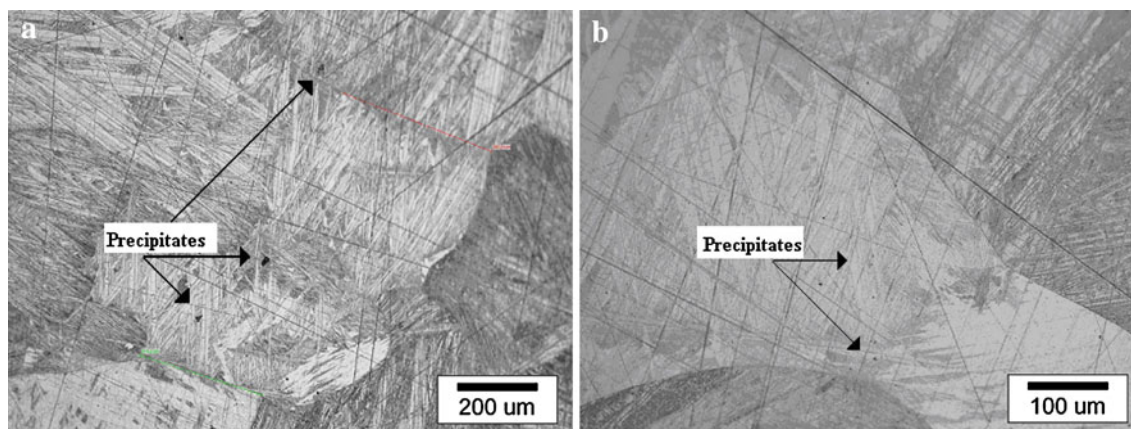


Fig. 3 Optical micrographs of the alloy; **a** 200 μm , **b** 100 μm

structure at room temperature (Fig. 3) and there are the precipitating-phases caused from the casting and generally called AlCu_3 (β_1) structures. A possible cause for the precipitation is the coalescence of the quenched in vacancies that is resulted in compositional gradients due to a local decrease in Al concentration. This favors the Al-rich precipitate formation at whose vicinity nucleation of martensite is occurred. The grain boundaries are definite, and each grain has different martensite variants. These variants are V-type and needle-type variants [15].

The differential scanning calorimetry measurements of the as-quenched sample were taken from the non-equilibrium room temperature β_1 to 250 $^\circ\text{C}$ with different heating rates of 10, 15, 20, and 25 $^\circ\text{C min}^{-1}$ and cooled down at the same rates. During heating, an endothermic reaction is occurred, transformation from martensite to austenite, whereas on cooling, an exothermic reaction is occurred, resulting in the reverse transformation from austenite to martensite. These reactions are indicated by the respective peaks in the plots. The endothermic peaks corresponding to martensite–austenite phase transformations of the alloy are shown in Fig. 4. The DSC scan features for the alloy exhibit a prominent multi-peak behavior only for the heating above 170 $^\circ\text{C}$. This feature can be referred to the pinning of the martensite by precipitates or to the multiple interfaces made transformation. High density of the precipitates restricts the mobility of the interfaces (austenite/martensite) during the transformation interval. Details of the transformation characteristics such as transformation temperatures and transformation hysteresis (A_f-M_s), transformation enthalpy and entropy were evaluated with the help of differential scanning calorimetry. The transformation temperatures such as austenite start A_s , austenite finish A_f , martensite start M_s , M_f martensite finish temperatures and transformation hysteresis values are given in Table 1. The measurement of transformation hysteresis defined as

$\eta(f_m = 0) = A_s-M_f$ and $\eta(f_m = 1) = A_f-M_s$ is shown in Fig. 5. It is seen that $\eta(1)$ and $\eta(0)$ are decreased continuously with decreasing heating and cooling rate. The heating/cooling rate sensitivity of the hysteresis measurement is clearly due to the delay of finishing temperatures of the transformations [17–20].

The changes in the transformation temperatures, which are concerned with the phases, are related to the thermodynamic parameters. The data obtained from the DSC measurements enables the determination of enthalpy and entropy values of the martensitic and austenitic transformations. The peaks recorded during heating, and cooling was integrated as a function of temperature. The total area of the peak from martensite to austenite (endothermic) or austenite to martensite (exothermic) gives the enthalpy ΔH . The entropy change occurred during these transformations can be given by the following equations;

$$\Delta S_{M \rightarrow A} = \frac{\Delta H_{M \rightarrow A}}{T_0} \quad (1)$$

or

$$\Delta S_{A \rightarrow M} = \frac{\Delta H_{A \rightarrow M}}{T_0} \quad (2)$$

where ΔS is the entropy change, ΔH is the enthalpy change, and T_0 is the equilibrium temperature [21]. The equilibrium temperature according to Salzbrenner and Cohen is determined by the following relation [22];

$$T_0 = \frac{1}{2}(M_s + A_f) \quad (3)$$

M_s is the martensite start temperature and A_f is the austenite finish temperature. The energy consists of two components, chemical energy and reversible mechanical energy, and T_0 is the temperature at which the chemical energies of austenite and martensite phases are balanced. In general,

Fig. 4 The DSC plot of the alloy measured with different heating/cooling rates

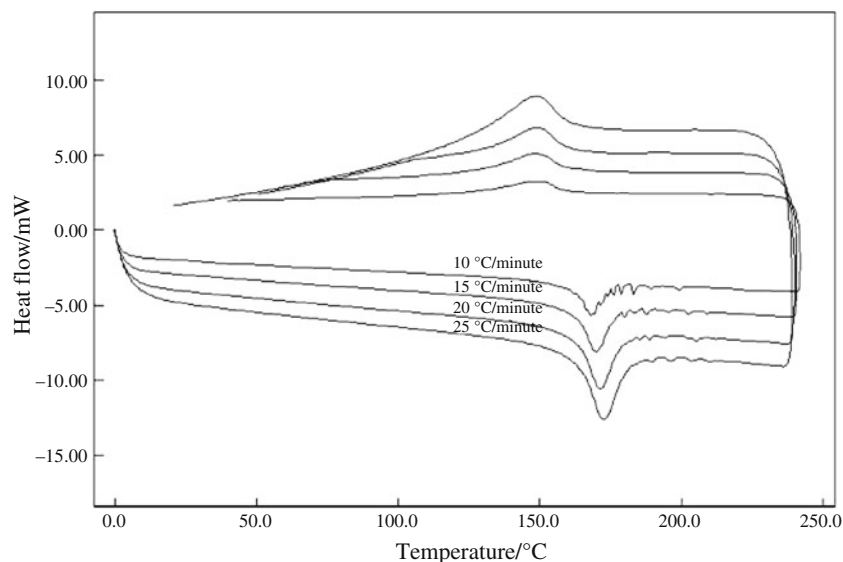


Table 1 The transformation temperatures and transformation hysteresis values of the of CuAlBe SMA alloy

Heating rate/°C min ⁻¹	A _s /°C	A _f /°C	A _{max} /°C	M _s /°C	M _f /°C	M _{max} /°C	Hysteresis (A _f -M _s)/°C	Hysteresis (A _s -M _f)/°C
10	157.5	174.7	168.1	159.5	124.4	148.9	15.2	33.1
15	160.2	178.5	170.2	159.6	122.6	149.3	18.9	37.6
20	161.6	180.2	171.1	159.5	128.0	148.3	20.7	33.6
25	162.0	183.8	173.0	162.9	122.4	149.1	20.9	39.6

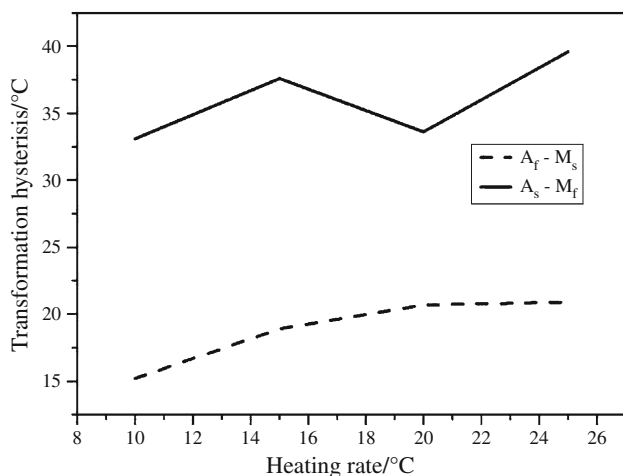


Fig. 5 Effect of heating and cooling rate on temperature hysteresis

the equilibrium temperature T_0 is expressed by Gibbs free energy relation;

$$\Delta G = \Delta H - T\Delta S \quad (4)$$

$$\Delta G^{A \rightarrow M} = 0 \text{ and } \Delta G^{M \rightarrow A} = 0 \text{ for } T = T_0 \quad (5)$$

This estimation can be approximated as follows [23–25]:

$$\Delta G^{A \rightarrow M} = G^M - G^A = \Delta H^{A \rightarrow M} - T\Delta S^{A \rightarrow M} \quad (6)$$

All the calculated values of the equilibrium temperatures, enthalpy and entropy changes of austenite and martensite transformations are given in Table 2.

The obtained DSC peaks and characteristic temperatures serve as a basis for determining kinetic parameters, i.e., activation energy of the process of martensitic and reverse transformation. The activation energy can change certainly with the temperature or take on negative values [26]. Since

Table 2 The equilibrium temperatures, enthalpy and entropy changes of austenite and martensite transformations of the CuAlBe SMA

Heating rate/°C min ⁻¹	T_0 /°C	$\Delta H_{M \rightarrow A}$ /Jg ⁻¹	$\Delta S_{M \rightarrow A}$ /Jg ⁻¹ °C ⁻¹	$\Delta H_{A \rightarrow M}$ /Jg ⁻¹	$\Delta S_{A \rightarrow M}$ /Jg ⁻¹ °C ⁻¹
10	167.1	6.94	0.041	-5.47	-0.033
15	169.05	7.10	0.042	-5.42	-0.032
20	169.8	7.15	0.042	-5.17	-0.030
25	173.3	7.20	0.041	-10.6	-0.061

Fig. 6 Activation energy curves of the alloy; **a** Kissinger, **b** Ozawa methods

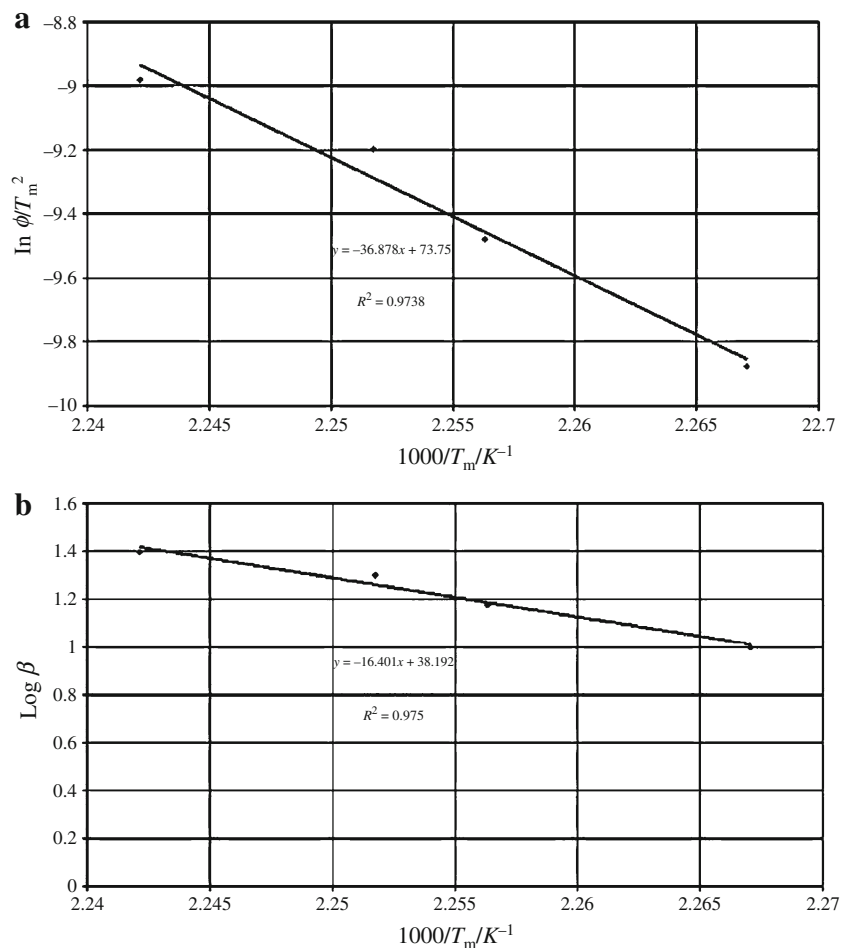
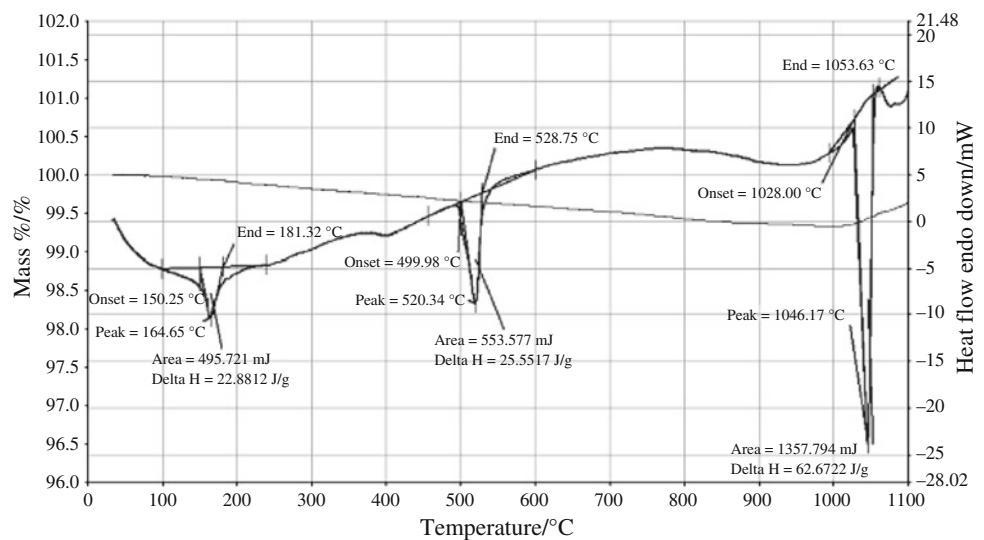


Fig. 7 TG/DTA curve of the alloy at a heating rate of $20\text{ }^\circ\text{C min}^{-1}$



various rates of heating and cooling are used for determining activation energy, the methods of Kissinger and Ozawa lead to linear relationships for martensitic and

reverse transformation as well (Fig. 6a, b). The results are processed according to the method developed by Kissinger [27]:

$$\frac{d \left[\ln \left(\frac{\phi}{T_m} \right) \right]}{d \left(\frac{1}{T} \right)} = \frac{-E}{R} \quad (7)$$

where ϕ is the heating rate, T_m the maximum on the DSC peak, R is the universal gas constant, and E is the activation energy and Ozawa [28]:

$$E = \frac{-R}{b} \left[\frac{d(\log \beta)}{d \left(\frac{1}{T_m} \right)} \right] \quad (8)$$

where b is a constant (0.4567), T_m the maximum on DSC peak, and E is the decomposition activation energy. The calculated activation energy values of the two different methods are 306.53 and 298.57 kJ mol⁻¹, respectively. The obtained activation energy values are close to each other.

The TG/DTA measurements were performed from room temperature to 1,100 °C at a heating rate of 20 °C min⁻¹. As seen in Fig. 7, there are three different phase transitions occurring at different temperatures. The decomposition of α -phase and the order–disorder transition of the parent-phase (DO₃ → B2) occurred near the eutectoid temperature. A single ordering transition in the Cu–Al–Be β -phase, from B2 to DO₃ structure, occurs under cooling at around 527 °C for low Be content and compositions near the eutectoid, with no significant dependence on the Be content [29, 30]. The peak observed nearly 400 °C is the transformation of CuAl₂-phase in the alloy and the result of this transformation the alloy became soften. The peak at around 800–1,000 °C is due to the liquefaction of the alloy. The general behavior of the Cu–Al–Be alloy was qualitatively similar as regards to the phase transformation sequence. Besides this, Fig. 7 shows the TG/DTA curve obtained from heating.

Conclusions

The microstructural and thermal analysis of Cu-14.82wt% Al-0.4wt% Be shape memory alloy were studied by microstructural observations and differential thermal analysis methods.

X-ray diffraction allows the determination of the phase of the grains of the polycrystalline sample. It was observed that the parent-phase ordered and has 18R martensite structure. This result was supported by the optical micrographs of the alloy which was obtained at room temperature. The grain boundaries and precipitate phases are seen in detailed from the micrographs. Each grain has different martensite variants. DSC measurement was used to investigate the austenitic–martensitic transformation temperatures and enthalpy upon continuous heating. The calculated values of the

entropy from austenite to martensite transformation are increased with the increasing heating rates. The activation energies of the alloy were calculated according to Kissinger and Ozawa methods, the results accommodate to each other. The sequence of the phase transition taking place in the studied alloy is B2 → DO₃ → 18R, so we can say that the sample has DO₃ austenitic and 18R martensitic-phase structure.

Acknowledgements This study is financially supported by TÜBİTAK, Project No.: 106T583.

References

1. Mallik U, Sampath V. Influence of aluminum and manganese concentration on the shape memory characteristics of Cu–Al–Mn shape memory alloys. *J Alloy Compd.* 2008;459:142–7.
2. Hsu CA, Wang WH, Hsu YF, Rehbach WP. The refinement treatment of martensite in Cu-11.38 wt% Al-043 wt% Be shape memory alloys. *J Alloy Compd.* 2009;474:455–62.
3. Montecinos S, Cuniberti A, Sepulveda A. Grain size and pseudoelastic behaviour of a Cu–Al–Be alloy. *Mater Charact.* 2008;59:117–23.
4. Silva RAG, Machado ES, Adorno AT, Magdalena AG, Carvalho TM. Completeness of β -phase decomposition reaction in Cu–Al–Ag alloys. *J Therm Anal Calorim.* 2012;109:927–31.
5. Kainuma R, Satoh N, Liu XJ, Ohnuma I, Ishida K. Phase equilibria and Heusler phase stability in the cu-rich portion of the Cu–Al–Mn system. *J Alloy Compd.* 1998;266(1–2):191–200.
6. Liu XJ, Ohnuma I, Kainuma R, Ishida K. Phase equilibria in the cu-rich portion of the Cu–Al binary system. *J Alloy Compd.* 1998;264:201–8.
7. Magdalena AG, Adorno AT, Silva RAG, Carvalho TM. Effect of Ag concentration on the thermal behavior of the Cu-10 mass % Al and Cu-11 mass % Al alloys. *J Therm Anal Calorim.* 2009;97(1):47–51.
8. Montecinos S, Cuniberti A, Castro ML, Boeri R. Phase transformations during continuous cooling of polycrystalline β -Cu–AlBe alloys. *J Alloy Compd.* 2009;467(1–2):278–83.
9. Montecinos S, Cuniberti A. Thermomechanical behavior of a CuAlBe shape memory alloy. *J Alloy Compd.* 2008;457:332–6.
10. Castro ML, Romero R. Isothermal decomposition of the Cu-22.72 Al-3.55 Be at.% alloy. *Mat Sci Eng-A Struct.* 2000;A287:66–71.
11. Montecinos S, Cuniberti A, Castro ML. Kinetics of isothermal decomposition in polycrystalline β CuAlBe alloys. *Intermetallics.* 2010;18(1):36–41.
12. Silva RAG, Adorno AT, Magdalena AG, Carvalho TM, Stipcich M, Cuniberti A, Castro ML. Thermal behavior of the Cu-22.55 at.% Al alloy with small Ag additions. *J Therm Anal Calorim.* 2011;103:459–63.
13. Marcos J, Manso L, Planes A, Romero R, Castro ML. Kinetics of the phase separation in Cu–Al–Mn alloys and the influence on martensitic transformations. *Philos Mag.* 2004;84(1):45–68.
14. Aksu Canbay C. The production of Cu-based shape memory alloys and investigation of microstructural, thermal and electrical properties of alloys, Ph.D Thesis. Firat University, Institute of Science, Elazığ/Turkey (Turkish) 2010.
15. Chentouf SM, Bouabdallah M, Cheniti H, Eberhardt A, Patoor E, Sari A. Ageing study of Cu–Al–Be hypoeutectoid shape memory alloy. *Mater Charact.* 2010;61:1187–93.
16. Lu X, Chen F, Li W, Zheng Y. Effect of Ce addition on the microstructure and damping properties of Cu–Al–Mn shape memory alloys. *J Alloy Compd.* 2009;480:608–11.

17. Suresh N, Ramamurty U. Effect of aging on mechanical behavior of single crystal Cu–Al–Ni shape memory alloys. *Mat Sci Eng-A Struct.* 2007;A454–455:492–9.
18. Suresh N, Ramamurty U. Aging response and its effect on functional properties of Cu–Al–Ni shape memory alloys. *J Alloy Compd.* 2008;499:113–8.
19. Perez-Landazabal JI, Recarte V, Sanchez-Alarcos V, No ML, San Juan J. Study of stability and decomposition of the β phase in Cu–Al–Ni shape memory alloy. *Mat Sci Eng-A Struct.* 2006;438–440: 734–7.
20. Meng Q, Yang H, Liu Y, Nam T. Transformation intervals and elastic strain energies of B2–B19 martensitic transformation of NiTi. *Intermetallics.* 2010;18:2431–4.
21. Prado MO, Decorte PM, Lovey F. Martensitic transformation in Cu–Mn–Al alloys. *Scripta Metall Mater.* 1995;33(6):878–83.
22. Salzbrenner RJ, Cohen M. On the thermodynamics of thermoelastic martensitic transformations. *Acta Metall.* 1979;27(5):739–48.
23. Kato H, Yasuda Y, Sasaki K. Thermodynamic assessment of the stabilization effect in deformed shape memory alloy martensite. *Acta Metall.* 2011;59:3955–64.
24. Ortin J, Planes A. Thermodynamic analysis of thermal measurements in thermoelastic martensitic transformations. *Acta Metall.* 1988;37:1873–89.
25. Obrado E, Manosa L, Planes A. Influence of composition and thermal treatments on the martensitic transition of Cu–Al–Mn alloys. *J Phys IV. France 7 (1997) Colloque C5, Supplement au Jour. De Phys. III de Novembre.*
26. Vyazovkin S, Burnham AK, Criado JM, Perez-Maqueda LA, Popescu C, Sbirrazzuoli N. ICTAC kinetics committee recommendations for performing kinetic computations on thermal analysis data. *Thermochim Acta.* 2011;20:1–19.
27. Kissinger HE. Reaction kinetics in differential thermal analysis. *Anal Chem.* 1957;29(11):1702–6.
28. Ozawa T. Kinetic analysis of derivative curves in thermal analysis. *Anal Calorim.* 1970;2(3):321–4.
29. Cuniberti A, Montecinos S, Lovey FC. Effect of gamma(2)-phase precipitates on the martensitic transformation of a β -CuAlBe shape memory alloy. *Intermetallics.* 2009;17(6):435–40.
30. Aksu Canbay C, Aydoğdu A. Thermal and microstructural properties of Cu–Al–Be shape memory alloys, Turkish Physical Society 27th International Physics Congress, İstanbul-Türkiye, Eylül 2010.